

A Measurement of xF_3^ν - $xF_3^{\bar{\nu}}$ and R with the CCFR Detector *

U. K. Yang, S. Avvakumov, P. de Barbaro, A. Bodek, H. Budd, D. A. Harris, K. S. McFarland, W. K. Sakumoto^a, R. A. Johnson, M. Vakili, V. Wu^b, C. G. Arroyo, A. O. Bazarko, J. M. Conrad, J. A. Formaggio, J. H. Kim, B. J. King, S. Koutsoliotas, W. C. Lefmann, C. McNulty, S. R. Mishra, A. Romosan, F. J. Sciulli, W. G. Seligman, M. H. Shaevitz, P. Spentzouris, E. G. Stern, B. M. Tamminga, A. Vaitaitis^c, R. H. Bernstein, L. Bugel, M. J. Lamm, W. Marsh, P. Nienaber, J. Yu^d, T. Adams, A. Alton, T. Bolton, J. Goldman, M. Goncharov, D. Naples^e, L. de Barbaro, D. Buchholz, H. Schellman, G. P. Zeller^f, J. Brau, R. B. Drucker, R. Frey, D. Mason^g, T. Kinnel, W. H. Smith^h

^aDepartment of Physics and Astronomy, University of Rochester, Rochester, NY 14627

^bDepartment of Physics, University of Cincinnati, Cincinnati, OH 45221

^cDepartment of Physics, Columbia University, New York, NY 10027

^dFermi National Accelerator Laboratory, Batavia, IL 60510

^eDepartment of Physics, Kansas State University, Manhattan, KS 66506

^fDepartment of Physics and Astronomy, Northwestern University, Evanston, IL 60208

^gDepartment of Physics, University of Oregon, Eugene, OR 97403

^hDepartment of Physics, University of Wisconsin, Madison, WI 53706

We report on a measurement of the neutrino-nucleon and antineutrino-nucleon differential cross sections in the CCFR detector. The measurement of the differential cross sections over a wide range of energies allows $\Delta xF_3 = xF_3^\nu - xF_3^{\bar{\nu}}$ and R to be extracted. ΔxF_3 is related to the difference between the contributions of the strange and charm seas in the nucleon to production of massive charm quark. The results for ΔxF_3 are compared to various massive charm NLO QCD models. The Q^2 dependence of R for $x < 0.1$ has been measured for the first time. [PREPRINT FERMILAB-Conf-99/193-E, UR-1574, ER-40685-934]

1. Introduction

Wide band neutrino beams provide an unique opportunity to measure R , the ratio of the longitudinal and transverse structure functions, and the difference between xF_3^ν and $xF_3^{\bar{\nu}}$. A measurement of R provides a test of perturbative QCD at large x , and probes the gluon density at small x . A non-zero $\Delta xF_3 = xF_3^\nu - xF_3^{\bar{\nu}}$ originates from the difference between the contributions of the strange and charm seas in the nucleon to massive charm quark production. Thus, a measurement of ΔxF_3 can be used to extract the strange

sea, and to understand massive charm production in neutrino-nucleon scattering. Previously, information on the strange sea came from the exclusive dimuon events channel ($\nu N \rightarrow \mu^- cX$, $c \rightarrow \mu^+ X'$) [1]. The dimuon analysis requires both an understanding of charm fragmentation and an acceptance correction for the detection of muons from charm decays. In previous extractions of structure functions [2], a leading order slow rescaling correction for heavy charm production was applied in order to extract a theoretically corrected F_2^ν which could be directly compared with F_2^μ . However, because of theoretical uncertainties in the treatment of massive charm production [3], this correction is no longer applied

*To be published in proceedings of the 7th International Workshop on Deep Inelastic Scattering and QCD, Zeuthen, Germany, Apr. 1999.

in this analysis. Furthermore, the value of $\Delta x F_3$ plays a crucial role in the extraction of F_2 at low x , where there is a long-standing discrepancy [2] between CCFR and NMC F_2 data. Therefore, it is important to measure the structure functions without any model-dependent slow rescaling corrections.

2. The CCFR experiment

The CCFR experiment collected data using the Fermilab Tevatron Quad-Triplet wide-band ν_μ and $\bar{\nu}_\mu$ beam. The CCFR detector [4] consists of an unmagnetized steel-scintillator target calorimeter instrumented with drift chambers, followed by a toroidally magnetized muon spectrometer. The hadron energy resolution is $\Delta E/E = 0.85/\sqrt{E}(\text{GeV})$, and the muon momentum resolution is $\Delta p/p = 0.11$. By measuring the hadronic energy (E_h), muon momentum (p_μ), and muon angle (θ_μ), we construct three independent kinematic variables x , Q^2 , and y . The relative flux at different energies obtained from the events with low hadron energy ($E_h < 20$ GeV) is normalized so that the neutrino total cross section equals the world average $\sigma^{\nu N}/E = (0.677 \pm 0.014) \times 10^{-38} \text{ cm}^2/\text{GeV}$ and $\sigma^{\bar{\nu} N}/\sigma^{\nu N} = 0.499 \pm 0.005$ [2]. The total data sample used for the extraction of structure functions consists of 1,030,000 ν_μ and 179,000 $\bar{\nu}_\mu$ events after fiducial and kinematic cuts ($E_\mu > 15$ GeV, $\theta_\mu < 0.150$, $E_h > 10$ GeV, and $30 \text{ GeV} < E_\nu < 360$ GeV). Dimuon events are removed because of the ambiguous identification of the leading muon for high- y events.

3. Measurement of differential cross sections

The differential cross sections are determined in bins of x , y , and E_ν ($0.01 < x < 0.65$, $0.05 < y < 0.95$, and $30 < E_\nu < 360$ GeV). Over the entire x region, differential cross sections are in good agreement with NLO Mixed Flavour Scheme (MFS) [5] QCD calculation using the MRST [6] PDFs. This calculation includes an improved treatment of massive charm production. Figure 1 shows typical differential cross sections

at $E_\nu = 150$ GeV. Also shown are the prediction from a LO QCD model, which is only used in the calculation of acceptance and resolution smearing correction. The CCFR data exhibit a quadratic y dependence at small x for neutrino and anti-neutrino, and a flat y distribution at high x for the neutrino cross section. Note that the y distributions of the CDHSW [7] differential cross sections data do not agree with those of CCFR data, or with the MRST predictions (this difference is crucial in any QCD analysis).

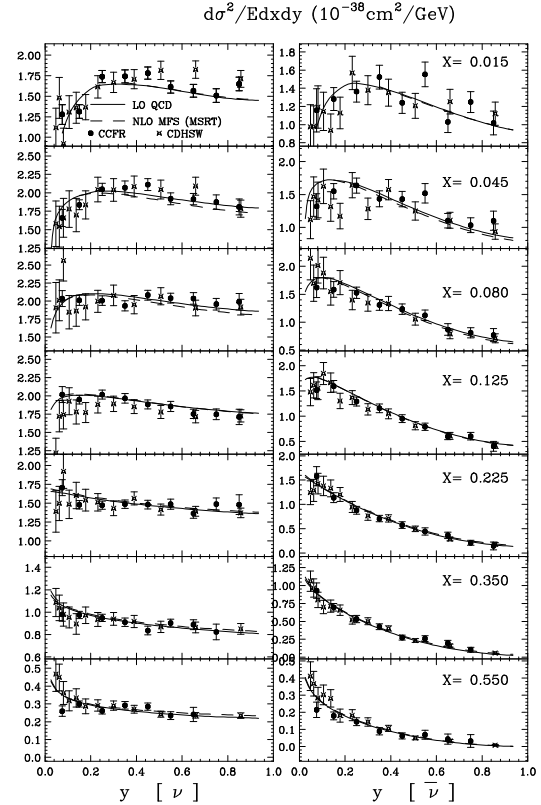


Figure 1. Preliminary CCFR differential cross section data at $E_\nu = 150$ GeV (both statistical and major systematic errors are included for the CCFR and CDHSW data). There is good agreement with the NLO MFS QCD calculation using MRST PDFs, and with LO QCD model which is used in the CCFR Monte Carlo. A disagreement is observed in the y distribution between CCFR data and CDHSW data.

4. Measurement of ΔxF_3 and R

Values of ΔxF_3 and R are extracted from the sums of neutrino and anti-neutrino differential cross sections. The sum of the two differential cross sections can be written as:

$$\begin{aligned} F(\epsilon) &\equiv \left[\frac{d^2\sigma^\nu}{dx dy} + \frac{d^2\sigma^{\bar{\nu}}}{dx dy} \right] \frac{(1-\epsilon)\pi}{y^2 G_F^2 M E} \\ &= 2xF_1[1 + \epsilon R] - \frac{y(1-y/2)}{1+(1-y)^2} \Delta xF_3 \end{aligned}$$

where $\epsilon \simeq 2(1-y)/(1+(1-y)^2)$ is the polarization of virtual W boson. To fit ΔxF_3 , R , and $2xF_1$ at a given x and Q^2 is very challenging because of the strong correlation between the ΔxF_3 and R terms, unless the full range of ϵ is covered by the data. Covering this range (especially the low ϵ region corresponding to high y) is difficult because of the low acceptance at high y .

Since the contribution of ΔxF_3 to $F(\epsilon)$ increases with Q^2 while that from R decreases, our strategy is to fit ΔxF_3 and $2xF_1$ for $Q^2 > 5$ where the ΔxF_3 contribution is relatively larger, constraining R with R_{world} [8]. (ΔxF_3 fits are done only for $x < 0.1$, because its contribution is small for $x > 0.1$.) It is reasonable to use R_{world} (an empirical fit for all available R data), because above $Q^2 = 5$, R for neutrino and muon scattering are expected to be the same, and R_{world} is in good agreement with the NMC muon data [9].

In the $Q^2 < 5$ region, where the contribution from R is larger, we fit R and $2xF_1$ with ΔxF_3 constrained to the model predictions. This allows us to study the Q^2 dependence of R for neutrino scattering at low Q^2 . In the $Q^2 > 5$ region, we test which scheme is favored for the massive charm treatment, based on the extracted ΔxF_3 results. Then the favored scheme is used in constraining ΔxF_3 for the $Q^2 < 5$ analysis.

Before the structure function extraction, we apply an electroweak radiative correction (Bardin) and corrections for the W boson propagator, and a non-isoscalar target (the 6.85% excess of neutrons over protons in iron; this effect is valid only at high x). The values of ΔxF_3 and R are sensitive to the energy dependence of the neutrino flux, but are insensitive to the absolute normalization. The uncertainty on the flux shape is estimated by using the constraint that F_2 and xF_3 should be flat over y (or E_ν) for each x and Q^2 bin.

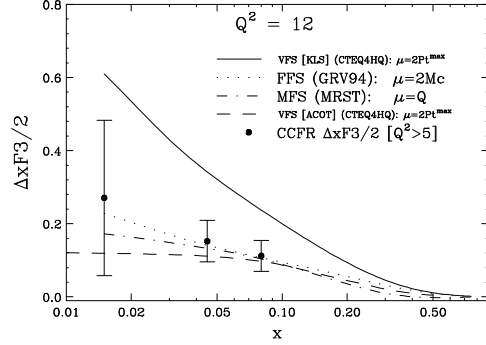


Figure 2. Preliminary CCFR ΔxF_3 data as a function of x compared with various schemes for massive charm production: KLS's VFS with CTEQ4HQ, FFS with GRV94, MFS with MRST, and ACOT's VFS with CTEQ4HQ

In the ΔxF_3 fit, we use the NLO MFS calculation with MRST PDFs for the Q^2 dependence of ΔxF_3 (for $Q^2 > 5$), and fit for the level of ΔxF_3 for each x bin below $x = 0.1$. Figure 2 shows the $\Delta xF_3/2$ data as a function of x . The CCFR data favor the Fixed Flavour Scheme (FFS) [10] calculation with the GRV94 [11] PDFs, and also the Mixed Flavour Scheme (MFS) using MRST PDFs. The data do not favor the VFS calculation with CTEQ4HQ [12] as implemented by Kramer, Lampe, and Spiesberger (KLS) [3]. The difference among the various schemes does not come from the different parton distributions, but rather from the different treatments of massive charm. In fact, all strange sea distributions in these parton distributions agree with the CCFR dimuon data [1]. Recently Olness and Kretzer [13] pointed out that KLS did not include the LO charm sea diagram in the VFS implementation, as required in the original ACOT's VFS calculation [14]. The ACOT's VFS calculations agree with data after the inclusion of the charm sea contribution, as shown in Fig. 2.

Since all three schemes except KLS' VFS show a good agreement with data, we use a MFS calculation with MRST PDFs (arguably the most reasonable theoretical description of massive charm production currently available) to constrain ΔxF_3 for the extraction of R for $Q^2 < 5$

and $x < 0.1$. Even for $Q^2 > 5$, we extract R in order to investigate its Q^2 dependence. The extracted values of R at fixed x vs Q^2 are shown in Fig. 3. The new data reveal the Q^2 dependence of R at $x < 0.1$ for the first time (R decreases as Q^2 increases for fixed x). The NMC data shown in Fig. 3 are integrated over Q^2 , and the two nearest NMC x bins are shown together. At higher x , our measurements agree with the other world data for R [8,9,15,16]. Figure 3 also shows a comparison with R_{world} with $m_c = 0$ (muon scattering or with slow rescaling correction in neutrino scattering) and $m_c = 1.3$ (without slow rescaling correction in neutrino scattering). The CCFR R data at $x = 0.015$ do not show R approaching zero as Q^2 goes zero (as expected in neutrino scattering, but not in electron scattering).

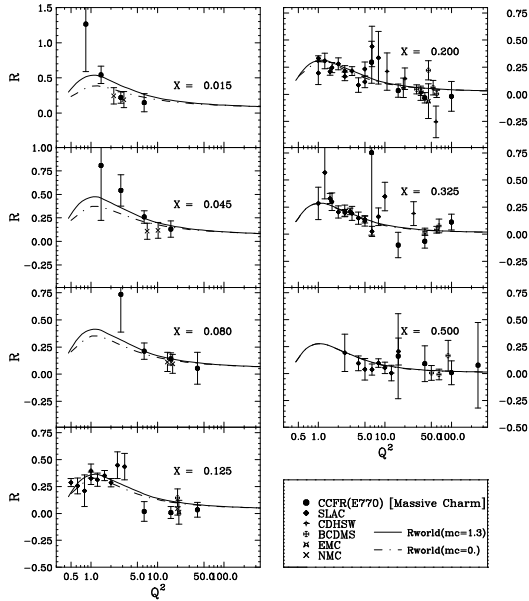


Figure 3. Preliminary CCFR R data as a function of Q^2 for various x , compared with other data and R_{world} with $m_c = 0$ and $m_c = 1.3$.

5. Conclusions

New measurements of $\Delta x F_3$ and R have been extracted from the CCFR differential cross sec-

tion data. The R data are extended to lower x and higher Q^2 than previous measurements. The Q^2 dependence of R at lower x region has been measured for the first time. The $\Delta x F_3$ data from $Q^2 > 5$ region agree with various schemes for the treatment of massive charm production. Further reduction of the errors in $\Delta x F_3$ is expected by including lower Q^2 data. The effect of $\Delta x F_3$ on the extraction of F_2 is currently under study. In addition, new data from the recent NuTeV run (1996-97), taken with sign selected neutrino beams, are expected to yield more precise determinations of $\Delta x F_3$, F_2 and R at low x .

REFERENCES

1. A. Bazarko *et al.*, *Zeit. Phys.* **C65**, 189 (1995).
2. W.G. Seligman *et al.*, *Phys. Rev. Lett.* **79**, 1213 (1997).
3. G. Kramer, B. Lampe, and H. Spiesberger, *Zeit. Phys.* **C72**, 99 (1996).
4. W.K. Sakumoto *et al.*, *Nucl. Instr. Meth.* **A294**, 179 (1991); B. King *et al.*, *Nucl. Instr. Meth.* **A302**, 254 (1991).
5. R.S. Thorne and R.G. Roberts, *Phys. Lett.* **B421**, 303 (1998).
6. A.D. Martin *et al.*, *Eur. Phys. J.* **C4**, 463 (1998).
7. P. Berge *et al.*, *Zeit. Phys.* **C49**, 607 (1991).
8. L.W. Whitlow *et al.*, *Phys. Lett.* **B250**, 193 (1990).
9. M. Arneodo *et al.*, *Nucl. Phys.* **B483**, 3 (1997).
10. E. Laenen, S. Riemersma, J. Smith, and W.L. van Neervan, *Nucl. Phys.* **B392**, 162 (1993).
11. M. Gluck *et al.*, *Zeit. Phys.* **C67**, 433 (1995).
12. H.L. Lai *et al.*, *Phys. Rev.* **D51**, 4763 (1995).
13. Private communication with F. Olness and S. Kretzer.
14. M. Aivazis, J. Collins, F. Olness, and W.K. Tung, *Phys. Rev.* **D50**, 3102 (1994).
15. L.H. Tao *et al.*, *Zeit. Phys.* **C70**, 387 (1996); S. Dasu *et al.*, *Phys. Rev.* **D49**, 5641 (1994).
16. J. Aubert *et al.*, *Nucl. Phys.* **B293**, 740 (1987); A. Benvenuti *et al.*, *Phys. Lett.* **237B**, 592 (1990).